# Letters

# Online Junction Temperature and Current Simultaneous Extraction for SiC MOSFETs With Electroluminescence Effect

Haoze Luo, *Member, IEEE*, Junjie Mao, *Student Member, IEEE*, Chengmin Li, *Member, IEEE*, Francesco Iannuzzo, *Senior Member, IEEE*, Wuhua Li, *Member, IEEE*, and Xiangning He, *Fellow, IEEE*

***Abstract*—In this letter, a junction-temperature and current extraction method is presented based on the electroluminescence mechanism of the SiC MOSFET body diode. Starting from the observation of two characteristic peaks in the emitted light spectrum, we proved that the junction temperature and the drain current can be simultaneously measured. This novel method consists of decoupling the relationship between the intensity of the electroluminescence peaks, the current, and the temperature. Through this optical method with inherent electrical isolation, the junction temperature and current in the SiC chip can be simultaneously measured with high precision. The total error of the junction temperature estimation is within ±3 °C, and the error of the current estimation is about ±0.2 A.**

***Index Terms*—Body diode, drain current, electroluminescence, junction temperature, SiC MOSFET.**

## I. Introduction

As a wide bandgap material, silicon carbide (SiC) has attracted widespread attention for its merits. In the field of high-voltage power electronics, SiC power MOSFETs are gradually replacing Si insulated-gate bipolar transistors (IGBTs) due to their higher switching speed and better figure of merit [1]. However, SiC technology also has some disadvantages, such as a higher power density, which challenges its interconnections, and a weak short-circuit tolerance. Therefore, fast and accurate detection of the junction temperature along with the current through the device is of key importance to ensure a safe and reliable operation [2].

Manuscript received April 26, 2021; revised May 31, 2021; accepted June 21, 2021. Date of publication July 7, 2021; date of current version September 16, 2021. This work was supported in part by the National Science Fund for Distinguished Young Scholars under Grant 51925702, in part by the Zhejiang Provincial Natural Science Foundation of China under Grant LQ21E070006, and in part by the Power Electronics Science and Education Development Program of Delta Group under Grant DREG20200002. Recommended for publication by Editor-in-Chief Y. Li. *(Corresponding authors: Chengmin Li; Wuhua Li.)*

Haoze Luo is with the College of Electrical Engineering, Zhejiang University, Hangzhou 310027, China, and also with the ZJU-Hangzhou Global Scientific and Technological Innovation Center, Zhejiang University, Hangzhou 310027, China (e-mail: haozeluo@zju.edu.cn).

Junjie Mao, Chengmin Li, Wuhua Li, and Xiangning He are with the College of Electrical Engineering, Zhejiang University, Hangzhou 310027, China (e-mail: maojunjie@zju.edu.cn; chengmin.li@epfl.ch; hxn@zju.edu.cn).

Francesco Iannuzzo is with the Department of Energy Technology, Aalborg University, 9220 Aalborg, Denmark (e-mail: fia@et.aau.dk).

Color versions of one or more figures in this article are available at https://doi.org/10.1109/TPEL.2021.3094924.

Digital Object Identifier 10.1109/TPEL.2021.3094924

Traditionally, a thermal-sensitive resistor with a negative temperature coefficient (NTC) is placed in the package to measure the temperature. However, due to the inevitably large distance between it and the target chip, the detection error is generally large as well. As a promising alternative, temperature-sensitive electrical parameters methods are now well established, which infer the junction temperature by measuring temperature-dependent electrical parameters, such as the ON-state resistance [3], di/dt during switching [4], the threshold voltage [5], and the turn-ON and turn-OFF delay time [6], [7]. However, high-voltage isolation requirements increase the difficulty of designing a measurement circuit which is electrically connected to the power module. On top of that, the sampled signal may be affected by the typical high electromagnetic interference environments of power electronic converters. In contrast, optical methods can achieve contactless measurements, but widely used instruments such as infrared imagers are too expensive and complex to be applied in the online junction temperature detection.

In the recent years, the electroluminescence phenomenon caused by the conduction of the SiC MOSFET body diode has been scientifically demonstrated [8]–[11]. Related research has shown that the luminescence intensity depends on the body diode current and the junction temperature, which paves the way for a new and promising sensing method. Worth noting, such methods provide inherent galvanic isolation by contactless detection. However, these articles have never investigated specifically the two characteristic peaks appearing in the emitted spectrum as a function of current and temperature. Besides, they all use an additional current sensor to decouple the junction temperature and forward current information from the measured light intensity. Worth noting, Kalker *et al.* [12] proposed to infer the junction temperature and current by using the artificial neural network. However, their work does not mention any way to decouple the current and the temperature, and it results relatively complex anyway in the online extraction.

In this letter, an analytical model correlating the two main energy peaks and current and temperature is established. In this way, we have proved that an estimation of both junction temperature and drain current can be achieved simultaneously and independently.

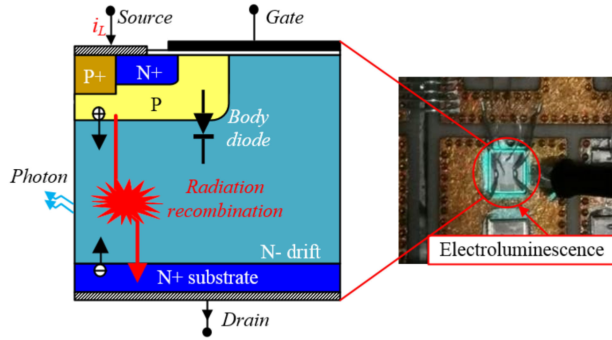


Fig. 1. Electroluminescence of SiC MOSFET.

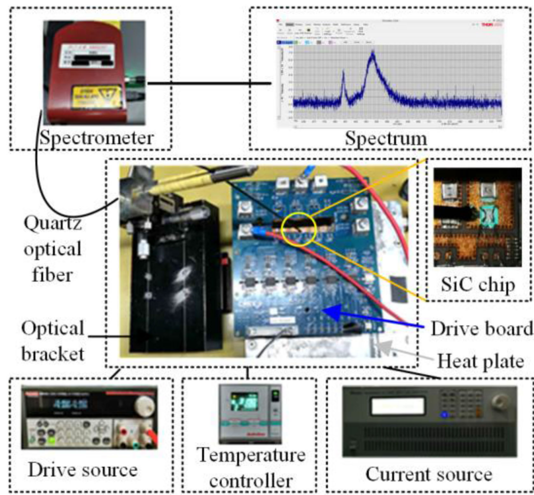


Fig. 2. Spectral calibration platform.

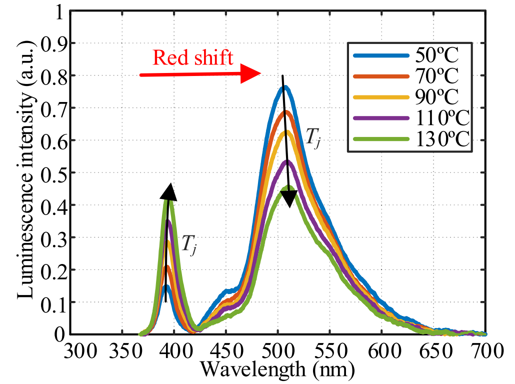


Fig. 3. Luminescence intensity under different temperatures at 9 A.

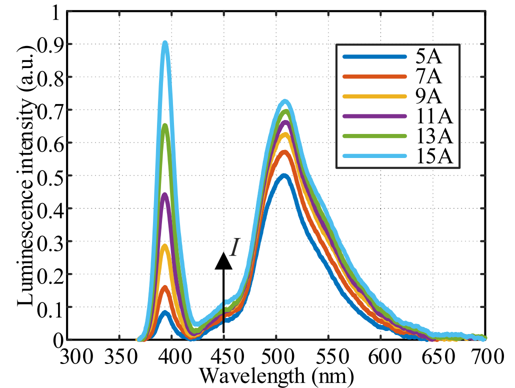


Fig. 4. Luminescence intensity under different currents at 90 °C.

## II. Electroluminescence of SiC MOSFET Body Diode

SiC MOSFET devices have an intrinsic P-i-N body diode operating in a bipolar conduction mode, as shown in Fig. 1. During its conduction, electrons and holes are injected into the low-doped region of the SiC MOSFET. Here, recombination occurs and there is a nonnegligible percentage of carriers that have the energy loss emitted in the form of photons, so-called radiation recombination. There are two kinds of radiation recombination processes observed in the low-doped region, including direct-band recombination and defect-energy-level recombination. The relationship between peak wavelength and recombination energy can be expressed as [13]

$$\lambda = \frac{hc}{E} \tag{1}$$

where $h$ is the Planck constant and $c$ is the light speed in the vacuum. For photons generated by the direct-band recombination, the peak wavelength roughly corresponds to the bandgap amplitude. The energy produced by defect-energy-level recombination is smaller than the bandgap, so its corresponding peak wavelength is higher than that produced by direct-band recombination.

To further investigate the discussed phenomenon of SiC MOSFET body diode, a test platform has been built as shown in Fig. 2. A Wolfspeed SiC MOSFET module CCS020M12CM2 is used for the tests. The anti-parallel Schottky diode is disconnected so that the current can directly flow through the MOSFET body diode. A negative gate voltage $V_{gs} = -5$ V is given to the gate using a driver board CGD15FB45P1 to keep the MOS channel under OFF state. A temperature-controlled heat plate is used to actively control the junction temperature. In the test, the body diode conducts with short current pulses of different values using a controllable-current source. The light emitted by the chip is brought to the spectrometer through a quartz fiber placed on the side of the SiC chip. The electroluminescence spectrum emitted under different conditions is analyzed using a Thorlabs CCS200 spectrometer.

The measured spectra under different temperatures at 9 A are displayed in Fig. 3. Two main peaks appear, namely the first one at 390 nm and the second one at 510 nm. Based on (1), the first one corresponds to the bandgap of 3.2 eV for 4H-SiC. The second one is likely to be caused by defect-energy-level recombination, which is commonly found in SiC crystals. Moreover, the first-peak intensity increases with temperature, whereas the second-peak intensity decreases with it. Besides, both peaks slightly shift toward red with increasing temperatures.

The measured spectrum under different currents at 90 °C is shown in Fig. 4. The intensities of both peaks increase with the current. Remarkably, the first-peak intensity increases much faster than the second peak.

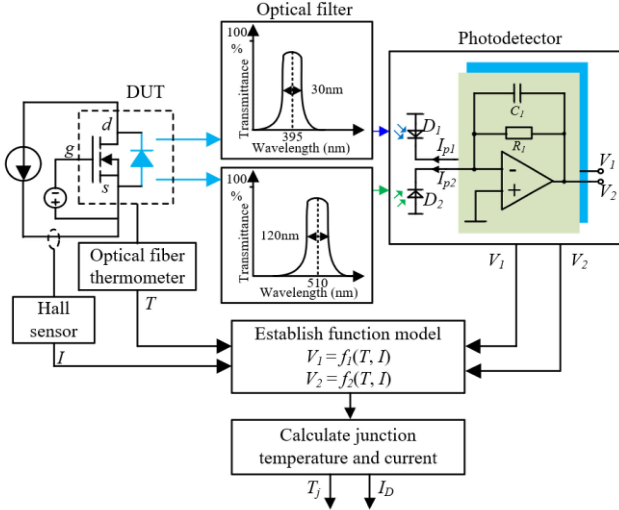


Fig. 5. Block diagram of the proposed junction-temperature and current-sensing approach. The SiC MOSFET is here indicated as device under test (DUT).

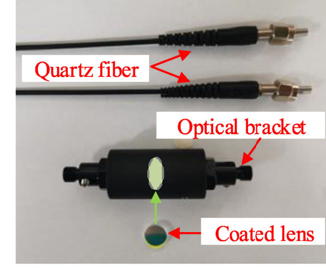


Fig. 6. Optical filter.

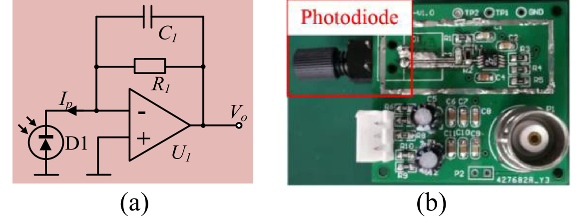


Fig. 7. Photodetector circuit. (a) Schematic diagram. (b) PCB board.

## III. Junction-Temperature and Current-Sensing Approach

The optical spectroscopy reveals that the spectrum varies with both the current and the temperature. The red-shift of the two characteristic peaks is a temperature-sensitive optical parameter that can be utilized for junction-temperature sensing. However, since the peak wavelength shift is only a few nanometers, a high-resolution spectrometer would be required for the high accuracy of $T_{\mathrm{j}}$ estimation. Therefore, this approach is not practical for junction temperature monitoring due to the high equipment cost.

It is worth noting that the electroluminescence intensity of the two characteristic peaks is both temperature-sensitive and current-sensitive. The first-peak intensity shows a positive temperature coefficient, whereas the second-peak intensity shows a NTC. Besides, the relationship between the two peak intensity and current is also significantly different. Therefore, in principle, both the junction temperature and the device current can be inferred by detecting the intensity of the two peaks, e.g., with photodetectors with different spectrum sensitivities, and then deconvoluting the response to work out the single contributions.

The block diagram of the junction temperature and load current-sensing approach is shown in Fig. 5. When the SiC MOSFET is in OFF-state and the load current flows through the body diode, electroluminescence occurs. The generated radiation is filtered through two band-pass optical filters with different transmission wavelengths to discriminate the first-peak and the second-peak. The optical filter is made up of a coated lens, an optical bracket, and quartz fibers as shown in Fig. 6. The coated lens installed in the optical bracket can transmit light in a specific wavelength band. The electroluminescence of the SiC chip is conveyed into the optical bracket through a quartz optical fiber, filtered by the coated lens, and then introduced into the photodetector through another quartz optical fiber. The output of the two optical filters is fed into two twin photodetectors and converted into output voltage, which is represented by $V_1$ and $V_2$. The conduction current $I$ of the body diode, junction temperature $T$ and the corresponding photoelectric voltages $V_1$ and $V_2$ need to be recorded under different working conditions for calibrating the analytical relationship, which can be expressed as

$$\begin{cases} V_1 = f_1(T, I) \\ V_2 = f_2(T, I) \end{cases}. \quad (2)$$

The above analytical model is fully identified using the measured data and a polynomial curve fitting algorithm. By inverting the system of (2), the SiC MOSFET current and its junction temperature can be simultaneously estimated.

TABLE I
Photodetector Parameters

| Symbol | Parameter |
|---|---|
| $R_1$ | 10 GΩ |
| $C_1$ | 0.1 pF |
| $D_1$ | SFH250V |
| $U_1$ | LTC6081 |

## IV. Experimental Verification

Due to the low emission efficiency of the SiC MOSFET body diode, it was necessary to design a high-gain photodetector as shown in Fig. 7. The parameters of the circuit are given in Table I. The promptness of this method depends on the bandwidth of the photodetector circuit. The bandwidth of the circuit in this letter can be expressed as

$$f_{\mathrm{BW}} = \frac{1}{2\pi R_1 C_1} = 159\,\mathrm{Hz}. \quad (3)$$

To verify the feasibility of the abovementioned junction-temperature and current extraction method, a forward current test was performed. A negative gate voltage $V_{\mathrm{gs}} = -5$ V was given to the gate. A step current was applied to the body diode through a controllable current source. The chip temperature of

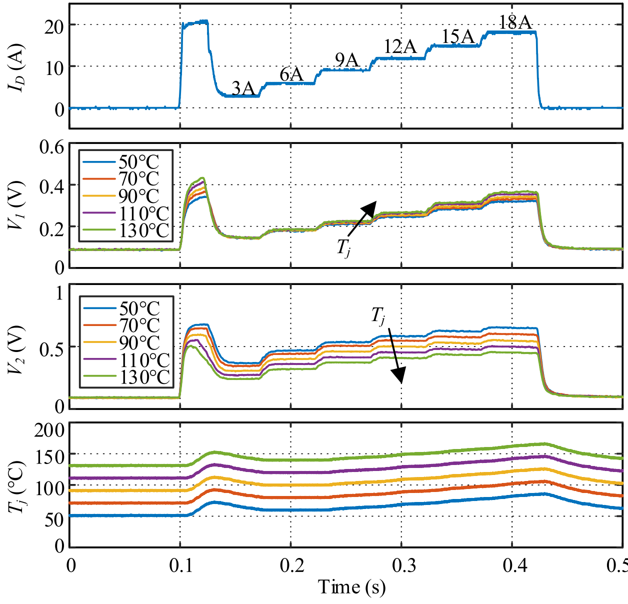


Fig. 8. Body diode forward current test: body diode current $I_D$; detected voltage of the first peak $V_1$; detected voltage of the second peak $V_2$; junction temperature $T_j$.

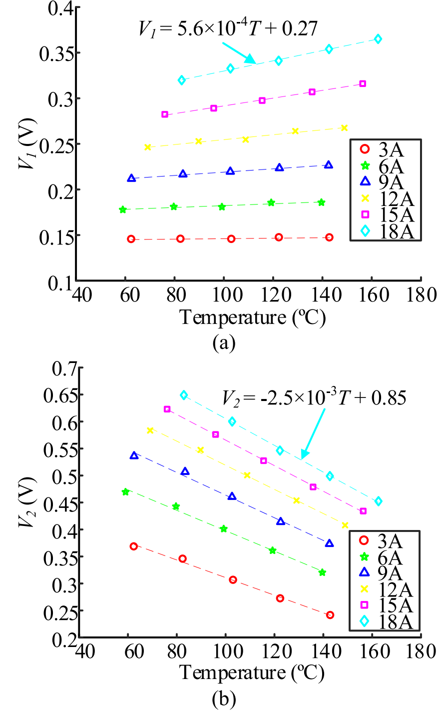


Fig. 9. Dependence of the detected voltage on temperature under different currents. (a) $V_1$. (b) $V_2$.

the SiC MOSFET was measured by a fiber optic sensor OpSens OTG-F. A Hall sensor CP9030H is used to detect the conduction current of the body diode. The substrate temperature of the SiC MOSFET module was regulated using a heating plate. The body diode of the SiC MOSFET was tested at several substrate temperatures: 50 °C, 70 °C, 90 °C, 110 °C, and 130 °C. A step current was applied, and the current value of each step was 3, 6, 9, 12, 15, and 18 A.

The test result is shown in Fig. 8. It can be seen that the output voltage $V_1$ of the first peak increases with conduction current and junction temperature. The output voltage $V_2$ of the second peak increases with conduction current but decreases with temperature. Due to the self-heating, the junction temperature $T_j$ increased by 35 °C by the current-conduction end. Therefore, when using the result of the forward conduction current test to establish an analytical model of the detected voltage, current, and temperature, the actual chip temperature needs to be used as the reference, rather than the substrate temperature. Besides, to reduce the interference of noise, temperature, current, and output voltage have been averaged over the steady intervals: 0.15–0.16 s, 0.2–0.21 s, 0.25–0.26 s, 0.3–0.31 s, 0.35–0.36 s, and 0.4–0.41 s.

As shown in Fig. 9, the detected voltage of the first-peak $V_1$ increases linearly with temperature, whereas the detected voltage of the second peak $V_2$ decreases linearly with temperature. Both the intercept and slope depend nonlinearly on the current. Therefore, the analytical model of detection voltage $V_1$ and $V_2$, current $I$, and temperature $T$ established by the polynomial curve fitting algorithm can be expressed as

$$\begin{aligned} V_1 &= (p_0 I^2 + p_1 I + p_2)T + p_3 I^2 + p_4 I + p_5 \\ V_2 &= (k_0 I^2 + k_1 I + k_2)T + k_3 I^2 + k_4 I + k_5 \end{aligned} \tag{4}$$

where $p_0 = 1.3 \times 10^{-6}, p_1 = 8.56 \times 10^{-6}, p_2 = -6.37 \times 10^{-6}$, $p_3 = -1.08 \times 10^{-4}, p_4 = 0.0109, p_5 = 0.111, k_0 = 2.69 \times 10^{-6}$, $k_1 = -1.1 \times 10^{-4}$, $k_2 = -1.33 \times 10^{-3}$, $k_3 = -8.99 \times 10^{-4}$, $k_4 = 0.0436$, and $k_5 = 0.354$. These coefficients were obtained based on the experimental results. A surface plot of (4) is shown in Fig. 10.

The process of solving the current can be reduced to finding the roots of

$$aI^4 + bI^3 + cI^2 + dI + e = 0 \tag{5}$$

where

$$\begin{aligned} a &= p_0 k_3 - k_0 p_3 \\ b &= p_0 k_4 + p_1 k_3 - k_0 p_4 - k_1 p_3 \\ c &= p_0(k_5 - V_2) + p_1 k_4 + p_2 k_3 - k_0(p_5 - V_1) - k_1 p_4 - k_2 p_3 \\ d &= p_1(k_5 - V_2) + p_2 k_4 - k_1(p_5 - V_1) - k_2 p_4 \\ e &= p_2(k_5 - V_2) - k_2(p_5 - V_1). \end{aligned} \tag{6}$$

The junction temperature can be calculated by substituting the calculated current into (4).

Fig. 11 shows the junction temperature and current calculated through the function model based on the forward current test results. In the electroluminescence stage, the calculated junction temperature and current quickly approach the measured values. When the current changes between 3 and 18A, the error between the calculated junction temperature and the measured junction temperature is within ±3 °C. The steady-state error between the calculated current and the measured current is within ±0.2 A.

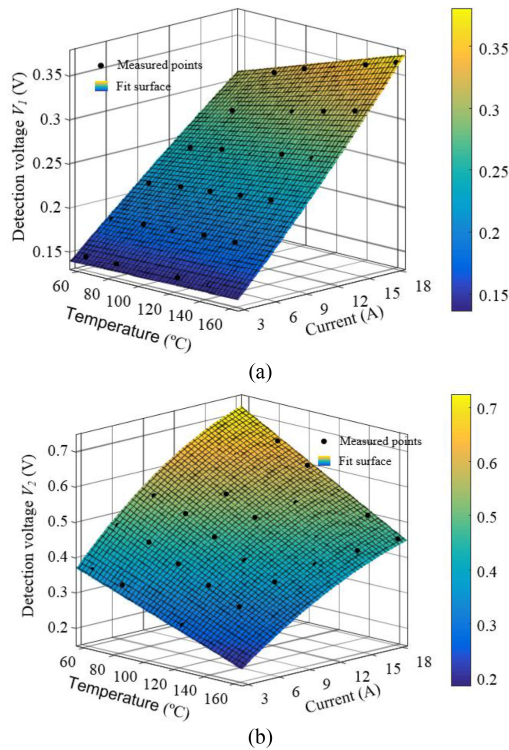


Fig. 10. 2D-surface plot of the used fitting function. (a) $V_1$. (b) $V_2$.

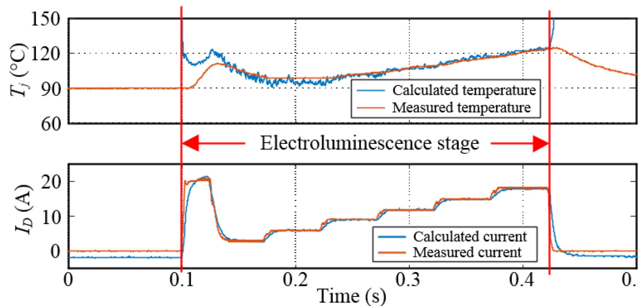


Fig. 11. Calculation results of junction temperature and current.

## V. Conclusion

The light emitted by the body diode of SiC MOSFETs has been profitably utilized to develop a galvanically isolated simultaneous junction-temperature and current-sensing method. By using optical filters with different transmission wavelengths and photoelectric amplifier circuits, the optical signals of the two emitted characteristic peaks have been detected. An analytical formulation was established by a polynomial curve fitting. By decoupling the function model, the junction temperature and the drain current of SiC MOSFET were inferred at the same time. The total error of the junction temperature estimation was within $\pm 3$ °C, and the error of the current estimation was within $\pm 0.2$ A.

## References


[1] J. Millan, P. Godignon, X. Perpina, A. Perez-Tomas, and J. Rebollo, "A survey of wide bandgap power semiconductor devices," *IEEE Trans. Power Electron.*, vol. 29, pp. 2155–2163, May 2014.

[2] S. Yang, A. Bryant, P. Mawby, D. Xiang, L. Ran, and P. Tavner, "An industry-based survey of reliability in power electronic converters," *IEEE Trans. Ind. Appl.*, vol. 47, pp. 1441–1451, May/Jun. 2011.

[3] F. Stella, G. Pellegrino, E. Armando, and D. Dapra, "Online junction temperature estimation of SiC power mosfets through on-state voltage mapping," *IEEE Trans. Ind. Appl.*, vol. 54, no. 4, pp. 3453–3462, Jul./Aug. 2018.

[4] J. O. Gonzalez, O. Alatise, J. Hu, L. Ran, and P. A. Mawby, "An investigation of temperature-sensitive electrical parameters for SiC power MOSFETs," *IEEE Trans. Power Electron.*, vol. 32, no. 10, pp. 7954–7966, Oct. 2017.

[5] A. Griffo, J. Wang, K. Colombage, and T. Kamel, "Real-time measurement of temperature sensitive electrical parameters in SiC power MOSFETs," *IEEE Trans. Ind. Electron.*, vol. 65, no. 3, pp. 2663–2671, Mar. 2018.

[6] B. Shi, S. Feng, L. Shi, D. Shi, Y. Zhang, and H. Zhu, "Junction temperature measurement method for power mosfets using turn-on delay of impulse signal," *IEEE Trans. Power Electron.*, vol. 33, pp. 5274–5282, Jun. 2018.

[7] Z. Zhang *et al.*, "Online junction temperature monitoring using intelligent gate drive for SiC power devices," *IEEE Trans. Power Electron.*, vol. 34, pp. 7922–7932, Aug. 2019.

[8] L. Ceccarelli, H. Luo, and F. Iannuzzo, "Investigating SiC MOSFET body diode's light emission as temperature-sensitive electrical parameter," *Microelectron. Rel.*, vol. 88–90, pp. 627–630, 2018.

[9] C. Li, H. Luo, C. Li, W. Li, H. Yang, and X. He, "Online junction temperature extraction of SiC power MOSFETs with temperature sensitive optic parameter (TSOP) approach," *IEEE Trans. Power Electron.*, vol. 34, no. 10, pp. 10143–10152, Oct. 2019.

[10] J. Winkler, J. Homoth, and I. Kallfass, "Electroluminescence-based junction temperature measurement approach for SiC power MOSFETs," *IEEE Trans. Power Electron.*, vol. 35, no. 3, pp. 2990–2998, Mar. 2020.

[11] G. Susinni, S. A. Rizzo, F. Iannuzzo, and A. Raciti, "A non-invasive SiC MOSFET junction temperature estimation method based on the transient light emission from the intrinsic body diode," *Microelectron. Rel.*, vol. 114, 2020, Art. no. 113845.

[12] S. Kalker, C. H. van der Broeck, and R. W. De Doncker, "Utilizing electroluminescence of SiC MOSFETs for unified junction-temperature and current sensing," in *Proc. IEEE Appl. Power Electron. Conf. Expo.*, 2020, pp. 1098–1105.

[13] D. A. Neamen, *Semiconductor Physics and Devices: Basic Principles*, 3rd ed. New York, NY, USA: McGraw-Hill, 2003.